Mathematical models of coagulation—are we there yet?

Received: 16 October 2023 | Revised: 24 February 2024 | Accepted: 12 March 2024

https://doi.org/10.1016/j.jtha.2024.03.009

ORIGINAL ARTICLE

Mathematical models of coagulation—are we there yet?

Matt J. Owen[1] | Joy R. Wright[2,3] | Edward G. D. Tuddenham[4] | John R. King[1] | Alison H. Goodall[2,3] | Joanne L. Dunster[5]

[1]Centre for Mathematical Medicine and Biology, School of Mathematical Sciences, University of Nottingham, Nottingham, United Kingdom

[2]Department of Cardiovascular Sciences, University of Leicester, Clinical Sciences Wing, Glenfield Hospital, Leicester, United Kingdom

[3]National Institute for Healthcare Research, Leicester Biomedical Research Centre, Glenfield Hospital, Leicester, United Kingdom

[4]Royal Free Hospital Haemophilia Centre, University College London, London, United Kingdom

[5]Institute for Cardiovascular and Metabolic Research, School of Biological Sciences, University of Reading, Reading, United Kingdom

Correspondence
Joanne L. Dunster, Institute for Cardiovascular and Metabolic Research, School of Biological Sciences, University of Reading, Whiteknights Campus, Reading RG6 6AS, UK.
Email: j.l.dunster@reading.ac.uk

Funding information
This work was supported by the Medical Research Council (MR/N013913/1, MR/W015293/1), the British Heart Foundation (RG/20/7/34866), and the Leverhulme Trust (fellowship). The recruitment and laboratory analysis of the Platelet Reactivity in Myocardial Infarction Study dataset were supported by the British Cardiac Society and the British Heart Foundation (PG/01/176), respectively.

Abstract

Background: Mathematical models of coagulation have been developed to mirror thrombin generation in plasma, with the aim of investigating how variation in coagulation factor levels regulates hemostasis. However, current models vary in the reactions they capture and the reaction rates used, and their validation is restricted by a lack of large coherent datasets, resulting in questioning of their utility.

Objectives: To address this debate, we systematically assessed current models against a large dataset, using plasma coagulation factor levels from 348 individuals with normal hemostasis to identify the causes of these variations.

Methods: We compared model predictions with measured thrombin generation, quantifying and comparing the ability of each model to predict thrombin generation, the contributions of the individual reactions, and their dependence on reaction rates.

Results: We found that no current model predicted the hemostatic response across the whole cohort and all produced thrombin generation curves that did not resemble those obtained experimentally. Our analysis has identified the key reactions that lead to differential model predictions, where experimental uncertainty leads to variability in predictions, and we determined reactions that have a high influence on measured thrombin generation, such as the contribution of factor XI.

Conclusion: This systematic assessment of models of coagulation, using large dataset inputs, points to ways in which these models can be improved. A model that accurately reflects the effects of the multiple subtle variations in an individual's hemostatic profile could be used for assessing antithrombotics or as a tool for precision medicine.

KEYWORDS
coagulation factors, kinetics, mathematical models, systems biology, thrombin

Manuscript handled by: Keith Neeves

Final decision: Keith Neeves, 13 March 2024

1 | INTRODUCTION

Coagulation results from a complex, tightly controlled set of reactions in plasma between the 6 core evolutionarily-related serine proteases (factor [F]II, FVII, FIX, FX, FXI, and FXII), 3 cofactors (FV, FVIII, and tissue factor [TF]), and 3 inhibitors (TF pathway inhibitor [TFPI], antithrombin [AT], and protein C), resulting in the generation of thrombin (Figure 1A [1,2]). In addition to these, there are proteins whose primary functions are outside of the coagulation cascade, such as the serpins alpha-1-antitrypsin, alpha-2-macroglobulin (α2-M), and alpha-2-antiplasmin, which can still alter the dynamics of thrombin generation. The many positive and negative checks and balances involved in the coagulation cascade result in thrombin being generated in the correct place and at the correct rate to ensure effective hemostasis. However, there is considerable variation in the levels of each factor in the plasma of individuals who have normal hemostatic response (Figure 1B), illustrating that it is the balance of the complex cascade that determines the overall hemostatic capacity of the plasma rather than the level of any 1 individual factor.

This overall coagulation response can be measured directly in the laboratory from the rate of thrombin generation in plasma using either a chromogenic or a fluorogenic substrate that is uniquely cleaved by thrombin [3–5]. This thrombin generation assay (TGA) essentially replicates the currently accepted, cell-based model of coagulation [6], with exogenous phospholipid (PL) and TF providing a substitute for the procoagulant surface of activated platelets and TF-bearing cells and microvesicles, respectively. The development of fully automated tools, such as ST Genesia (Diagnostica Stago) [7], allows clinical applications of the TGA to assess thrombotic potential in patients, allowing personalized treatments [8]. The TGA is plotted as a thrombin generation curve, which can be reduced into a handful of summary statistics (Figure 1C)—namely, the endogenous thrombin potential (ETP), which is the area under the thrombin generation curve; the peak height of thrombin generation and the time to reach this peak height, which provide information on the rate and magnitude of the response, respectively; and the lag time, which is the time to reach 5% of the peak thrombin concentration and approximates the traditional clotting time used clinically to test for bleeding defects.

Since the kinetics of the reactions of individual coagulation factors are generally well established, this enables an alternative approach to assessing thrombin generation using mathematical models. These capture, explain, and simulate the reactions that lead to thrombin generation using mathematical representations of the coagulation cascade (Figure 2A and Table [9–31]). Such models produce time-dependent predictions of the concentrations of all coagulation factors. They have been used to aid understanding of how the proteins interact [32] and are regulated [33] and to determine the key drivers of coagulation in both healthy subjects and patients with bleeding conditions [26,33–36]. Such models, if accurate, could also provide invaluable tools for assessing the effects of novel antithrombotic or therapeutic agents designed to prevent bleeding without the need for extensive experimentation.

This approach, largely pioneered by Mann et al. e.g. [11,16], has gained increasing engagement from mathematicians in recent years (Figure 2B). Several mathematical models of the coagulation cascade have been developed that vary in the reactions they capture and in the predictions they make, with models increasing in complexity alongside biological discoveries. Early models, such as that of Khanin and Semenov [9], comprised a limited number of reactions, focusing on FVII, FX, FV, and FII. The model subsequently proposed by Jones and Mann [11] contained a more complete version of the cascade but lacked the inhibitors AT, TFPI, and protein C. This group subsequently expanded their model to incorporate AT and TFPI [16], and this version has been frequently used as a baseline for further models by the same group [19,26,29] and others [25,28,30,31]. Some models were developed independently, placing emphasis on other parts of the coagulation cascade such as contact activation, PLs, protein C, and platelets [18,20–24,27].

These mathematical depictions of coagulation have been used to generate predictions [37] and test hypotheses [38], but their effectiveness has been debated [39,40]. Given that these models are validated against a single output (thrombin) under variation of few components, Hemker et al. [40] suggest that the reaction rates used to construct these models cannot be reliably determined by fitting these models to a thrombin generation curve. They highlighted key issues with the models, such as differences in their predictions for a typical thrombin generation curve, and highlighted the significant inconsistency in the reaction rates used for the same reactions between these models. Conversely, Mann [39] highlighted some uses for the models, emphasizing their cost effectiveness over experimentally derived data and high transparency for exploratory analysis. We agree that models can be useful tools but believe that they need to be validated extensively against large datasets that reflect the variation in the levels of all factors rather than only a single factor since the resulting predictions are a composite of variation in all factors.

One of the primary challenges in quantitative validation is obtaining sufficient data from single studies or data consistency if combining multiple datasets. This, along with the variation in values for thrombin generation between different laboratories, may be why there have been few studies in which these models have been validated against data from large numbers of healthy subjects or patients. A study that did investigate this is that of Chelle et al. [41], which used data from 112 subjects—40 hemophilia A patients, 40 hemophilia B patients, and 32 healthy male controls—and found that none of the models of thrombin generation they tested reproduced patient data. They did not investigate the potential reasons for this failure, and instead, they explored reparameterization of one of the models for individual donors.

Here, we focus on mathematical representations of the coagulation cascade that aim to simulate thrombin generation as it occurs *in vitro* under similar conditions to experimentally derived TGA data (Table). As such, we selected models that:

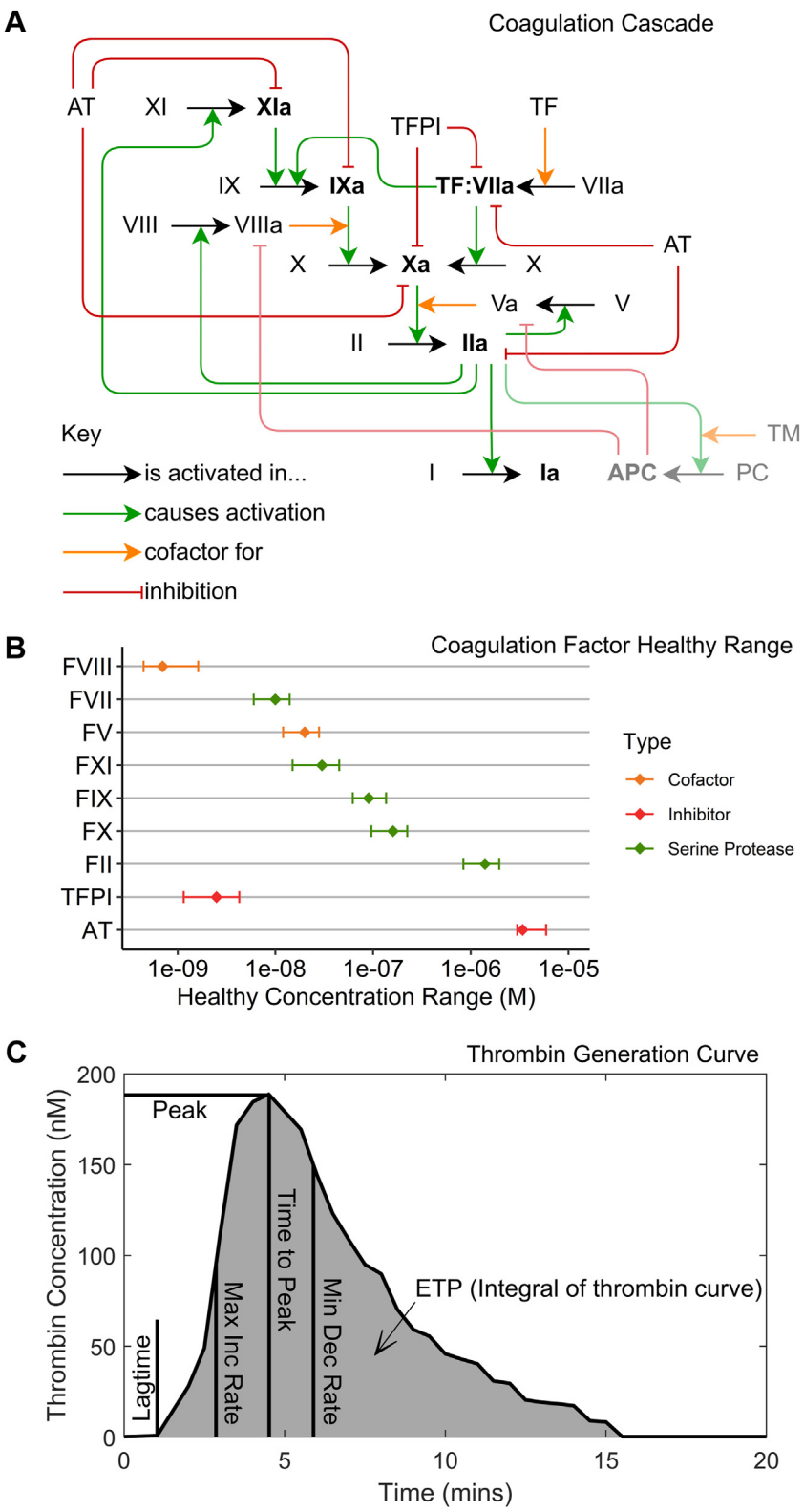

FIGURE 1 The coagulation cascade and thrombin generation curves. (A) A reaction network of the coagulation cascade under activation through the tissue factor (TF) pathway. The reactions for protein C (PC), shown in grey, are not included in the simulations here as they require cell-surface-bound thrombomodulin (TM) and endothelial PC receptor to be activated in significant amounts. (B) A forest plot of coagulation factor concentrations demonstrating typical ranges in healthy individuals. The levels for factor (F)XI are taken from Mohammed et al. [1], and all other healthy ranges and concentrations are from Danforth et al. [2]. (C) An example of a thrombin generation curve illustrating the summary statistics that can be derived. Peak and time to peak are the maximum thrombin concentration and the time to reach it, respectively. Lag time is the time to reach 5% of the peak height. Endogenous thrombin potential (ETP) is the integral of the thrombin generation curve. Maximum increasing rate (Max Inc Rate) and minimum decreasing rate (Min Dec Rate) are the largest positive and negative values of the gradient of the thrombin generation curve, respectively. APC, activated protein C; AT, antithrombin; TFPI, tissue factor pathway inhibitor.

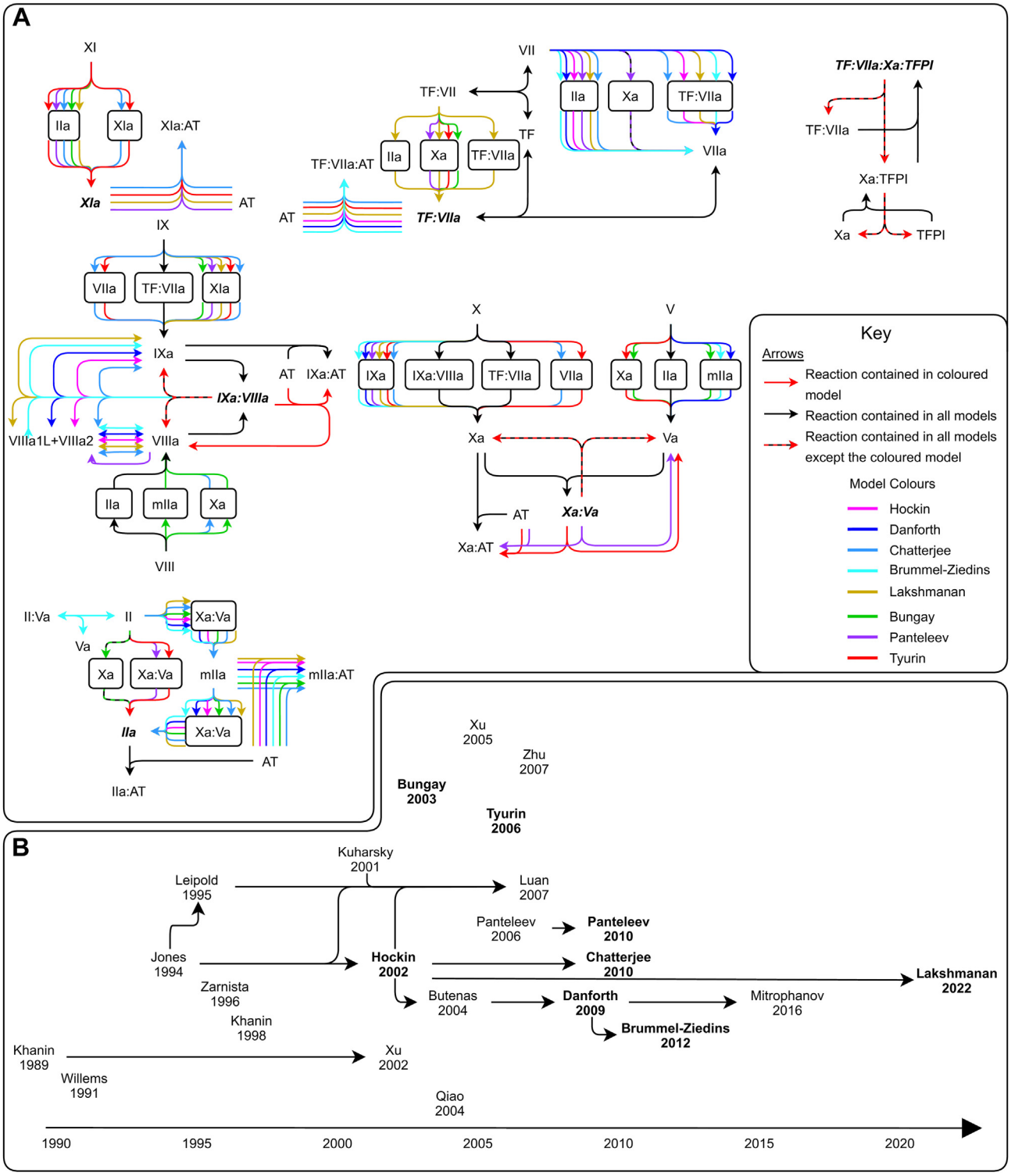

FIGURE 2 Current mathematical models of thrombin generation. (A) A comparison of the reactions captured in the simulated models. In all cases, reactions involving protein C, contact activation, alpha 1-antitrypsin, alpha 2-antiplasmin, alpha 2-macroglobulin, C1 inhibitor, plasminogen activation inhibitor-1, and Boc-VPR-MCA (Boc-Val-Pro-Arg-methylcoumarin amide; a fluorogenic substrate) have been removed. (B) A timeline depicting the development of mathematical models. Models simulated here are in bold. AT, antithrombin; TF, tissue factor; TFPI, tissue factor pathway inhibitor.

TABLE Details of *in vitro* thrombin generation models.

Model	TF pathway	Common pathway	XI	XII	AT	TFPI	PC	Platelets	Spatial
Khanin and Semenov [9]	VII	X, V, II	-	-	-	-	-	-	-
Willems et al. [10]	-	X, V, II	-	-	✓	-	✓	-	-
Jones and Mann [11]	TF, VII	X, V, II, IX, VIII	-	-	-	-	-	-	-
Leipold et al. [12]	TF:VIIa only	X, V, II, IX, VIII	-	-	-	-	-	-	-
Zarnitsina et al. [13]	-	X, V, II, IX, VIII	✓	-	✓	-	✓	-	-
Khanin et al. [14]	TF, VII	X, V, II, IX, VIII	-	-	✓	✓	-	-	-
Kuharsky and Fogelson [15]	TF, VII	X, V, II, IX, VIII	-	-	✓	✓	✓	✓	-
Hockin et al. [16]	TF, VII	X, V, II, IX, VIII	-	-	✓	✓	-	-	-
Xu et al. [17]	TF:VIIa only	X, V, II, IX, VIII	-	-	✓	✓	-	✓	-
Bungay et al. [18]	TF, VII	X, V, II, IX, VIII	✓	-	✓	✓	✓	-	-
Butenas et al. [19]	TF, VII	X, V, II, IX, VIII	-	-	✓	✓	-	-	-
Qiao et al. [20]	-	X, V, II, IX, VIII	-	-	-	-	✓	-	-
Xu et al. [21]	TF:VIIa only	X, II, IX, VIII	-	-	-	✓	-	-	-
Tyurin and Khanin [22]	TF, VII	X, V, II, IX, VIII	✓	✓	✓	✓	✓	-	-
Panteleev et al. [23]	TF, VII	X, V, II, IX, VIII	✓	-	✓	✓	✓	✓	✓
Zhu [24]	TF, VII	X, V, II, IX, VIII	✓	✓	✓	✓	✓	-	-
Luan et al. [25]	TF, VII	X, V, II, IX, VIII	-	-	✓	✓	✓	✓	-
Danforth et al. [26]	TF, VII	X, V, II, IX, VIII	-	-	✓	✓	-	-	-
Panteleev et al. [27]	TF, VII	X, V, II, IX, VIII	✓	-	✓	✓	✓	-	-
Chatterjee et al. [28]	TF, VII	X, V, II, IX, VIII	✓	✓	✓	✓	-	✓[a]	-
Brummel-Ziedins et al. [29]	TF, VII	X, V, II, IX, VIII	-	-	✓	✓	✓	-	-
Mitrophanov et al. [30]	TF, VII	X, V, II, IX, VIII	-	-	✓	✓	-	-	-
Lakshmanan et al. [31]	TF, VII	X, V, II, IX, VIII	✓	-	✓	✓	-	-	-

Models used in this investigation are shown in bold. Ticks represent factors that are included in the model.

AT, antithrombin; PC, protein C; TF, tissue factor; TFPI, tissue factor pathway inhibitor.

[a] Platelets are summarized using only a single parameter, and only minor effects of platelets are used.

- Contain a comprehensive description of the reactions from initiation through to the generation of thrombin (ie, include FX, FV, FII, FIX, and FVIII)
- Include a comprehensive description of cascade initiation, having both TF and FVII
- Contain the inhibitors AT and TFPI
- Neglect platelets, as the experimental data were collected using platelet-poor plasma
- Neglect protein C, or inclusion of protein C is optional, as the TGA lacks the cell surface endothelial protein C receptor that is required for effective activation of protein C
- Neglect spatial interactions, as the TGA occurs in a well-mixed *in vitro* environment

This led us to compare simulations from 8 published models, which we refer to using the first author's surname, namely, the models of Hockin [16], Danforth [26], Chatterjee [28], Brummel-Ziedins [29], Lakshmanan [31], Bungay [18], Panteleev [27], and Tyurin [22]. These models are represented by a large number of ordinary differential equations that include between 24 and 81 equations and between 42 and 110 parameters. It is worth noting that we excluded the models of Mitrophanov et al. [30] and Butenas et al. [19]. While they meet the above requirements, they have not been included in our analysis because of their similarity to the Danforth model. The models of Khanin et al. [14] and Zhu [24] also meet the requirements, but difficulties in implementing these models meant they were also removed.

To aid others in testing these models, we have provided complete descriptions, including their validation methods, reactions, and reaction rates for all the models used. These are given in the Supplementary Information alongside, for the first time for some of these models, links to download the code to run simulations.

We tested these models against measured values of coagulation factors and inhibitors from a large dataset from 348 donors from the Platelet Reactivity in Myocardial Infarction Study (PRAMIS) that comprises 162 patients who suffered a myocardial infarction (MI) at an early age (≤50 years) and 186 healthy donors matched for age,

self-reported male/female gender, and current smoking status [42,43]. The data comprise measured levels of coagulation FII, FV, FVII, FVIII, FIX, FX, FXI and inhibitors (TFPI and AT) [43] and ETP measurements from a chromogenic TGA [3]. This allowed us to compare the modeled thrombin generation outputs for all individuals to experimentally obtained ETP for the same samples. This large dataset allows testing and validation of each of the models against natural variation in coagulation factors, allowing evaluation of the accuracy of these models and identification of ways to improve them. We explored whether any of the models are able to predict laboratory-measured ETP. We show how these models perform in response to variation in levels of procoagulants and inhibitors, and finally, we show which parts of the coagulation cascade dominate model predictions.

2 | METHODS

2.1 | Experimental data

The demographics of the PRAMIS cohort have been described previously [42], as has the analysis of the hemostatic factors for each subject [43]. Here, we used data from a subset of the PRAMIS subjects (86% of the cohort) for whom coagulation factor levels and thrombin generation had been measured, comprising 162 patients (14% female) who suffered an MI up to the age of 50 years and 186 age-matched, gender-matched, and smoking status–matched healthy controls. The key data demographics of these subjects, which have been described in detail previously [43], are provided in Supplementary Table S1. While the MI patients were receiving aspirin, none of the subjects was being treated with antithrombotic medications or any drugs that would affect coagulation. The MI patients were sampled >6 months after their cardiovascular event, at a time when any hemostatic abnormalities related to their infarct event would have stabilized. Therefore, for this analysis, cases and controls were considered as a single group.

Blood was obtained in the morning from subjects in a fasting state and was collected by clean venepuncture via a 21-guage butterfly needle without tourniquet into 3.2% (w/v) citrate and processed within 10 minutes of collection. Plasma was prepared by centrifugation at 1800*g* for 30 minutes and stored in single-use aliquots at −80 °C until analysis. These conditions were standardized to minimize artifactual activation of the hemostatic system and to minimize contact activation during plasma preparation. The study was approved by the UK Leicestershire Health Authority Ethics Committee (reference 5506; project number RFL 472), and all subjects provided written informed consent. This study conformed to the Declaration of Helsinki and the principles of the Belmont report.

Plasma levels of the coagulation factors and inhibitors were measured for each subject as described previously [43]. Briefly, the coagulation FII, FVII, FVIII, FIX, FX, and FXI were measured by 1-stage turbidometric clotting assays using a Sysmex CA6000 coagulation analyzer (Sysmex) and deficient plasmas from Dade Behring (Milton Keynes). Clotting time was determined against a reference curve for each factor. AT was measured on the Sysmex CA6000 analyzer using an automated chromogenic method (Berichrom, Dade Behring). Data for these factors and inhibitors are expressed as a percentage by comparison to the protein standard for each factor. TF and TFPI activities were measured using chromogenic assays based on generation of FX activity (ADI), and the values were expressed in pM and units, respectively. These measured values, which have been reported previously [43] and are shown as box plots in Supplementary Figure S1, formed the inputs for the various mathematical models.

Laboratory measurement of thrombin generation was performed using a chromogenic assay, initiated with 4 μM PL and an additional 5 pM of TF [3]. The TGA provided a measure of ETP, which was compared to model outputs.

2.2 | Donor-specific simulations

To obtain model predictions for each of the 348 individuals, the donor-specific coagulation factor concentrations of FII, FV, FVII, FVIII, FIX, FX, FXI, and AT were used as model inputs. This produces model-predicted concentrations of all activated and nonactivated coagulation factors and complexes, most notably thrombin, over time.

We compared model-predicted ETP, derived from these patient-specific model-predicted thrombin generation curves, with the experimentally measured ETP. Model accuracy was measured through 2 metrics: R^2, which measured correlation between model-predicted and experimental ETP, reporting values between 0 (no linear correlation) and 1 (perfect linear correlation); and root mean squared error (RMSE), which gives a measure of the average error in the model predictions of ETP in units of percentage of pooled plasma. An RMSE between 5 and 10 would be considered good, and an RMSE of 0 means that the ETP of all individuals was predicted exactly. Further details are provided in the Supplementary Information and summarised in Supplementary Figure S2.

Simulations also yielded predictions for the full range of coagulation factors over time. As will be shown later, these predictions for a typical donor (coagulation factor concentrations in Supplementary Table S2) were compared to identify areas of agreement and disagreement between model reactions that lead to thrombin generation. Full model descriptions, including all reactions are reaction rates, are given in Supplementary Tables S4 to S18.

2.3 | Model sensitivity to variation in inputs

To understand how the predicted thrombin generation curves change with varying initial factor concentrations, we conducted a sensitivity analysis on each of the models. The concentration of each coagulation factor varied between 50% and 150% of their reference value, maintaining the others fixed at their reference concentration. A set of 6 summary statistics (lag time, peak height, time to peak, ETP, maximum increasing rate, and minimum decreasing rate; Supplementary Figure S3) were extracted from the resulting model-predicted thrombin generation curves and combined into a

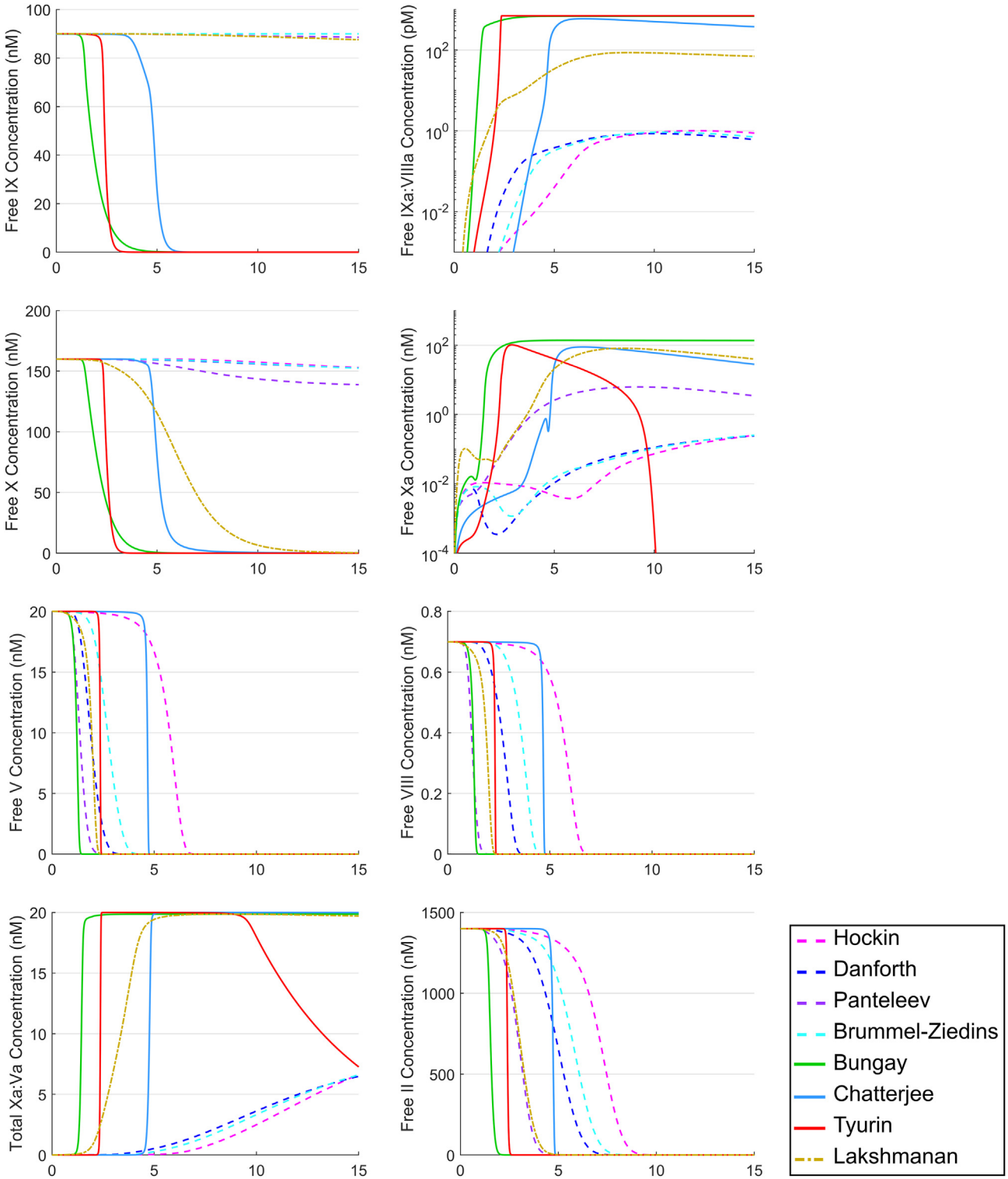

FIGURE 3 Formation of Xa and Xa:Va. Concentration curves for factor (F)IX, IXa:VIIIa, FX, FXa, FV, FVIII, and Xa:Va, demonstrating the differences in FIXa and FXa activation between the models. Models that fall into the Quick group are illustrated by solid lines, while those that fall into the Symmetrical group are shown as dashed lines.

single sensitivity value for each coagulation factor for each of the 8 models.

A similar approach was also used, varying the reaction rates used in each of the models. To demonstrate the sensitivity of model output to variation in these reaction rates, we grouped reactions into the groups TF:VIIa, Xa, Xa:Va, IIa, IXa, IXa:VIIIa, XIa, AT, and TFPI based on their subsidiary end product. For example, activation of FX is included within the Xa group, while activation

of FV and binding of FXa and FVa are in the Xa:Va group. The reactions in each group are provided in Supplementary Table S19. This allowed us to report a single sensitivity (the largest sensitivity) for each group.

Further details are provided in the Supplementary Information.

3 | RESULTS

3.1 | The models fail to capture the range in donor responses accurately

All 8 models were used to predict thrombin generation for the 348 donors, but while the models accurately predicted ETP for some donors, they failed to accurately predict the response for all (Figure 4). The RMSE values quantify the distance between model predictions and data and varied between 27.4 and 31.9, with the Panteleev model giving marginally the best result (RMSE = 27.4). There was no apparent difference in the accuracy of the model predictions between the males and females (shown in blue and red, respectively). Also, while there was a wider range of both measured and calculated ETP for the cases (open circles) compared with the controls (closed circles), the accuracy of the models does not appear to be significantly different between the 2 groups.

3.2 | The models vary in the shape of the thrombin generation curves they predict

In addition to determining the accuracy of the different models against the experimental ETP values, we explored the qualitative appearance of the thrombin generation curves that each model generated. For this, a fixed set of initial concentrations for a typical donor (Supplementary Table S2 [16]) was used to generate standard thrombin generation curves. As can be seen from this modeling (Figure 5A), there was little agreement in the shape and magnitude of the predicted thrombin generation curves, mirroring the findings of both Chelle et al. [41] and Hemker et al. [40], with only the Lakshmanan model reproducing the shape of a typical curve obtained experimentally. The Chatterjee and Tyurin models predicted a sharp, rapid onset of thrombin generation, albeit with very different lag times, while Hockin, Danforth, Brummel-Ziedins, and Panteleev predicted slower, more symmetrical curves. The Bungay model predicted a sharp early curve of substantially lower peak height, likely due to its larger rate of inhibition of FIIa by AT, which was 10 times faster than the rates utilized by other models. We separated the models (except Lakshmanan) into 2 groups (the Quick group included Chatterjee, Bungay, and Tyurin and the Symmetrical group included Hockin, Danforth, Brummel-Ziedins, and Panteleev) to identify the causes of these differences in shape.

In addition to these qualitative differences in predictions of thrombin generation, the models also predicted different ranges for the values of ETP across the dataset, ranging between 100 and 2000 nM·min. As an example, the model by Bungay predicted low levels for ETP (in the range of 100-250 nM·min), and Lakshmanan predicted very large ETP in excess of 6000 nM·min in some cases. The Hockin model predicted ETP in the range of 250 to 1250 nM·min, and the Tyurin model predicted ETP in the range of 750 to 1500 nM·min. The Panteleev model was unusual in that it predicted ETP in a narrow range centred around 1000 nM·min, while the remaining models predicted ETP to be in the range of 750 to 2000 nM·min. Experimentally determined ranges for healthy ETP appear comparable with those predicted by most of these models (1000-2000 nM·min [44]); however, the range for healthy ETP was still assay-specific, and all but the Bungay and Lakshmanan models reproduced healthy ranges observed in at least 1 other study [45,46].

Although, as shown in Figure 4, the models did not correlate well with the experimental ETP (R^2 = 0.13-0.20), they did correlate strongly with one another (Figure 5B; r values >0.8 for all pairings other than Hockin-Panteleev and Hockin-Tyurin). However, while the models all predicted ETP to be generally in the same region of their respective distribution range, this did not mean it was likely that the measured ETP for each donor was similar. Other summary statistics (such as peak, time to peak, and lag time) provided a much wider separation between model outputs, although models that shared very similar parameters, such as those of Danforth and Brummel-Ziedins, remained highly correlated through all summary statistics (r values of >0.99). Panteleev and Lakshmanan were also highly correlated with both Danforth and Brummel-Ziedins pairing (r values of >0.8). The distribution of these summary statistics is given in Supplementary Figure S4.

3.3 | The models vary in their predictions of the reactions that dominate thrombin generation

As pointed out by Hemker et al. [40], contrary to predictions from all of the models, prothrombin is not believed to be fully depleted *in vitro*. It has been shown that only around 90% of FII is converted to FIIa [47]. This discrepancy is in part related to the possible mechanisms attributed to the inhibition of the prothrombinase complex. Only the Tyurin and Panteleev models include a direct method of inhibition of Xa:Va by AT (Xa:Va + AT → Xa:AT + Va), while all other models require Xa:Va to disassociate before the FXa can be inhibited. This means that high levels of prothrombinase activity remain in these models for a significant amount of time, continuing activation of FII until it is all depleted. Inclusion of some form of direct prothrombinase inhibition is likely necessary in order for some prothrombin not to be converted, but its presence in the models of Tyurin and Panteleev that do include it does not appear to be sufficient since both models still converted all the prothrombin.

Figure 3 presents plots of the concentrations of various coagulation factors over time, focusing on FX and FIX. The predicted depletion of FX and FIX clearly separated into the same groups that were observed in the shapes of the thrombin generation curves. The Symmetrical group produced much smaller (by a factor of 1000) levels

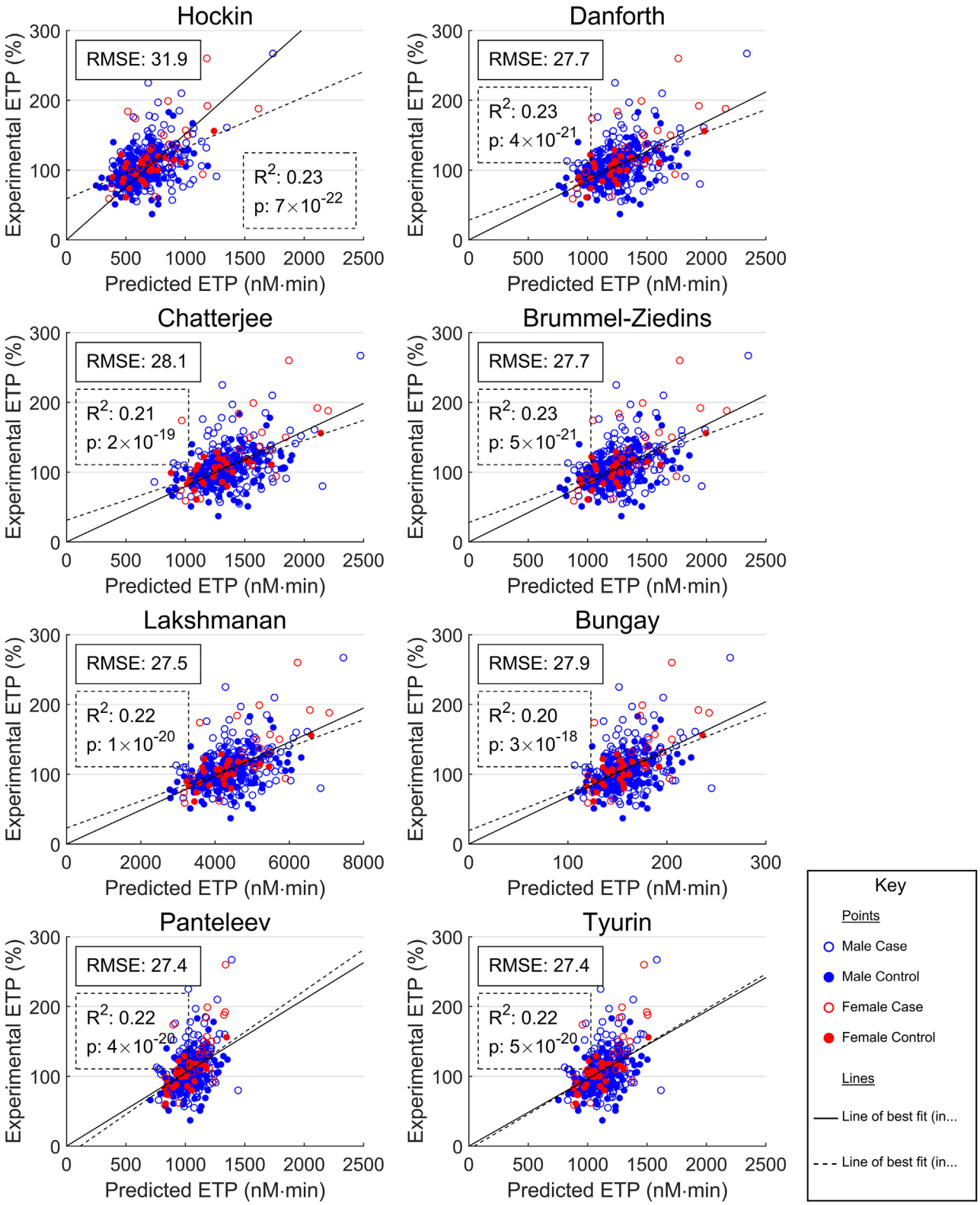

FIGURE 4 Comparisons of model predictions to data. Scatter plots of predicted endogenous thrombin potential (ETP, using the measured concentrations of coagulation factors in the dataset) against experimentally measured ETP in order to measure ETP correlation for each of the models. The root mean squared error (RMSE) is given for each model (a smaller RMSE represents a better fit); for comparison, a linear model (using coagulation factor concentrations to predict ETP; with 5-fold cross-validation to avoid overfitting) gives an RMSE of 25.5. RMSE measures error compared with the solid line of best fit; R^2 and *P* values for correlation are given for the hatched line of best fit.

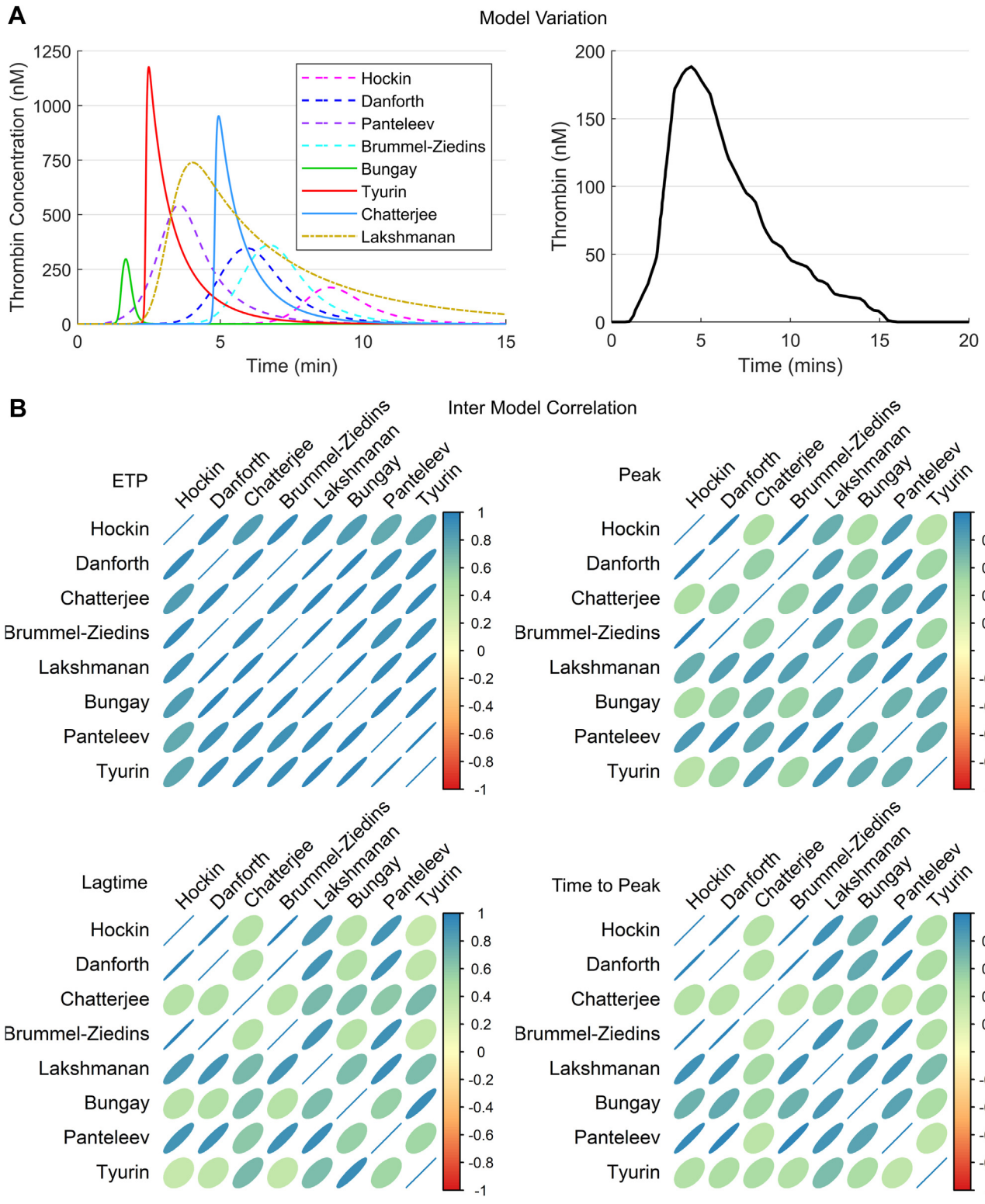

FIGURE 5 Variation in predicted thrombin generation curves. (A) The variation in predicted thrombin generation curves for the same baseline coagulation factors. The Quick group is demonstrated using a solid line, while the Symmetrical group uses a dashed line. An example of a realistic thrombin generation curve is given for comparison. (B) A cross-model comparison of predicted summary statistics. Correlograms (of correlation coefficient r) of each model's predictions for endogenous thrombin potential (ETP), peak, time to peak, and lag time using the scaled coagulation factors of all patients. The angle of the ellipse demonstrates whether the correlation between the 2 models, for that summary statistic, is positive or negative. The width of the ellipse (and the color) demonstrates the strength of the correlation (measured using the correlation coefficient r), where a wide ellipse demonstrates a weak correlation and a narrow ellipse demonstrates a strong correlation.

of IXa:VIIIa, which in turn caused lower levels of FXa to be generated, and consequently lower levels of Xa:Va, causing the differences in the thrombin generation curves. Since FV and FVIII are fully activated in all the models, with no clear separation between the 2 groups, then the levels of FXa and FIXa were the drivers of the differences in the production of Xa:Va and IXa:VIIIa between the models.

We identified the primary cause of the shape of the thrombin generation curves in the Quick group, the models that demonstrated rapid thrombin generation, to be high levels of FIXa. The Quick group all featured FXI, which may explain why they fully activated FIX, a fact that is not achieved by the Symmetrical group of models. The Panteleev model also includes FXI, though the activation of FIX is much weaker than the models in the Quick group (Panteleev, $k_{cat}/K_m = 4.9 \times 10^5 M^{-1}s^{-1}$; Chatterjee, $k_{cat}/K_m = 1.6 \times 10^7 M^{-1}s^{-1}$), resulting in far less FIX and, subsequently, FX activation. This is demonstrated clearly in Figure 6, where FXI is removed from the models, which strongly affected the models of Bungay, Tyurin, and Chatterjee, reducing the sharp onset of the curve that characterized the Quick group, while the model of Panteleev did not change significantly, as expected.

While the Lakshmanan model does feature FXI, it does not fully activate FIX, so activation of FX is more gradual (albeit still fully depleted), resulting in this model falling between the Quick and Symmetrical groups. Figure 6 suggests that, in this model, FXI activation is only relevant for low TF concentrations [31].

3.4 | The models have differential responses to changes in plasma levels

The results of the coagulation factor–based sensitivity analysis are shown in Figure 7A. The sensitivities are reported as proportions, split across each model. The maximum sensitivity value for a coagulation factor is 1, in which case only that coagulation factor changes the thrombin generation curve, and all other sensitivities for that model will be 0. The larger the sensitivity value, the greater the change in the summary statistics and, therefore, the effect on the thrombin generation curve.

Unsurprisingly, the thrombin generation curves of all models were sensitive to the initial concentrations of FII and AT. The Hockin, Danforth, Brummel-Ziedins, Panteleev, and Lakshmanan models gave similar sensitivities with low sensitivity to FV and higher sensitivity to TF, with Bungay and Tyurin reporting the reverse (low TF and high FV). Chatterjee was the only model sensitive to FXI.

3.5 | Models differ in their response to changes in reaction rates

Since the literature reports variable different rates for various reactions, this was also explored using a sensitivity analysis. Figure 7B gives a heat map of the sensitivity of the models to changes in their reaction rates between 50% and 150% of their given values. The Chatterjee model was the only model sensitive to FXI reactions. The Hockin, Danforth, and Brummel-Ziedins models all had a similar distribution of sensitivities, with AT being the most sensitive and Xa:Va being the least. Chatterjee's modifications to the Hockin model produced a very different sensitivity distribution with an even larger focus on AT and a reduced focus on the initiation of the cascade, with lower sensitivities for TF:VIIa, FXa, and TFPI.

All models exhibited FIIa inhibition by AT as the most sensitive reaction, the same reaction identified by Hemker to contain a wide variation in values used between different models [40]. This reaction dominated the Bungay and Panteleev models, where only reactions involving AT or FIIa produced any significant variation, whereas the remaining models still showed some significant variation caused by other reactions.

4 | DISCUSSION

Constructing a mathematical model of the coagulation cascade consists of 3 challenging tasks. The first is to identify the reactions and interactions that occur in the cascade, considering emerging information on new interactions, for example, the recent description of inhibition of

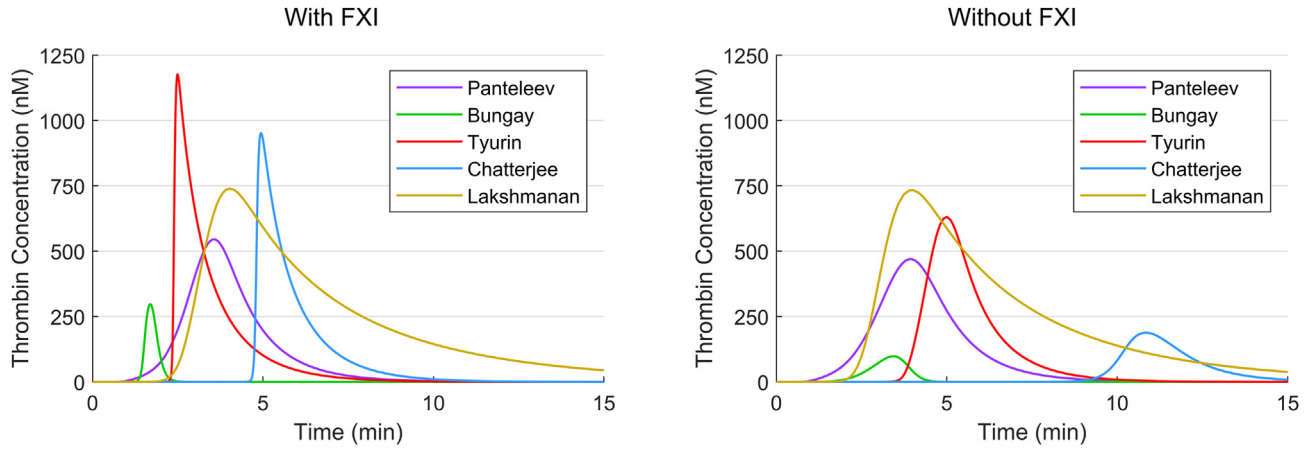

FIGURE 6 The effect of factor (F)XI on model predictions. Thrombin generation curves, both with and without FXI, for the 5 models that include FXI demonstrating the influence of FXI over model output.

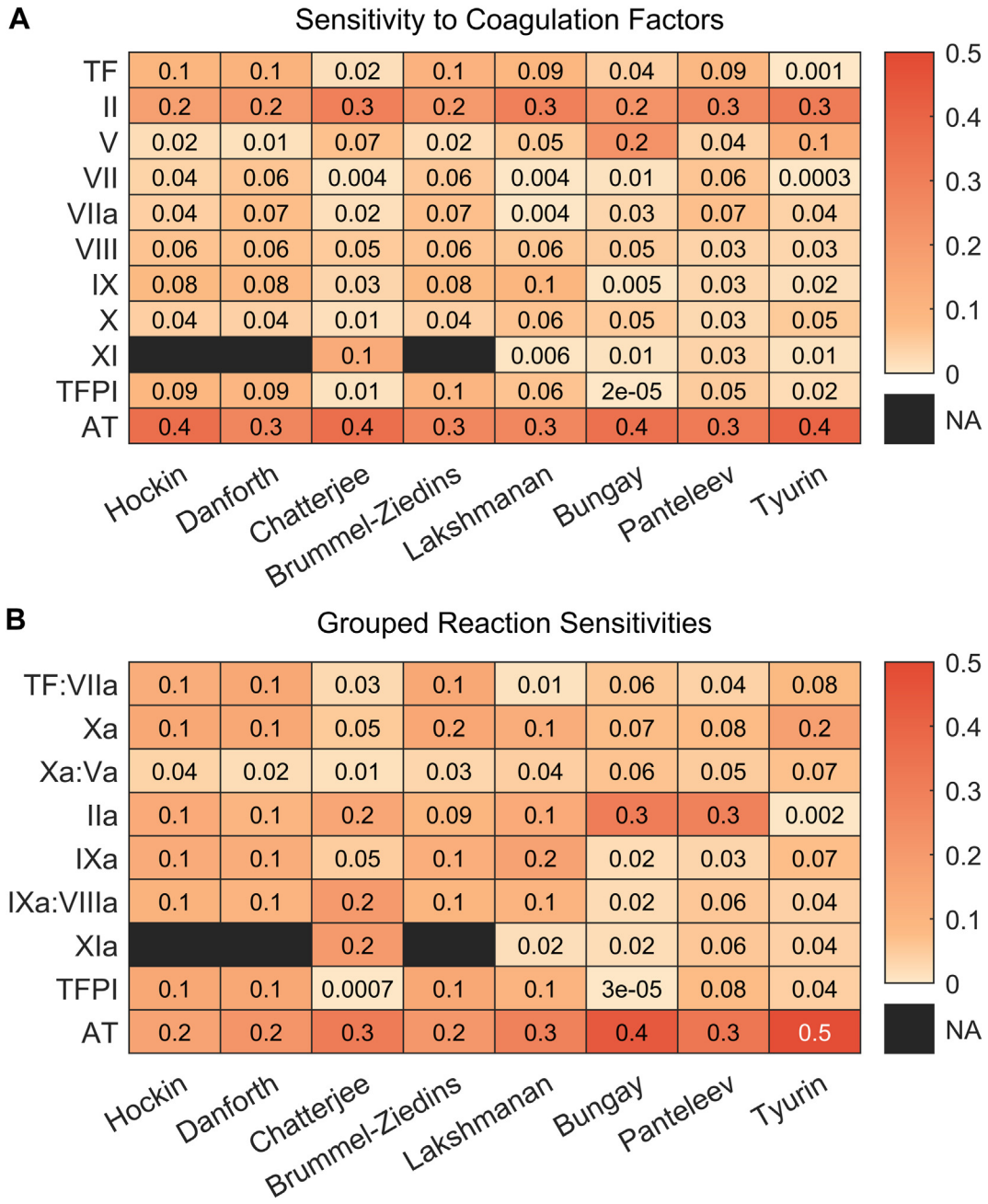

FIGURE 7 Sensitivity of each model to levels of each coagulation factor. (A) Heat map of sensitivity to the initial concentration of various coagulation factors. A high sensitivity (given in red) demonstrates that variation in that coagulation factor has a significant effect on the thrombin generation curves predicted by that model. (B) Heat map of reaction sensitivities. Each reaction rate is placed into a group based on the reaction's function in the cascade (formation of tissue factor [TF]:VIIa, factor [F]Xa, Xa:Va, FIIa, FIXa, IXa:VIIIa, and FXIa; inhibition by antithrombin [AT]; and inhibition by TF pathway inhibitor [TFPI]) and the maximum reaction-rate sensitivity for that group is given in the heat map. A high sensitivity (given in red) demonstrates that there is a reaction rate in that group whose variation has a significant effect on the thrombin generation curves predicted by that model. NA, not applicable, and indicates that a model does not include a specific coagulation factor or any reactions in the given group.

FXa generation by FVa [48] or the interactions between protein S and TFPI [49–51]. The second is to identify the rates for each of these reactions, with even the simplest models requiring the specification of over 30 rate constants. The choice of a rate constant is not simple since experimentally obtained rates in the literature vary by orders of magnitude [40], largely due to variation in the experimental conditions used to generate the data [41]. Additionally, the lack of availability of rate constants for more recently discovered reactions, such as between protein S and TFPI, hampers their inclusion into mathematical models [50,51]. The third challenge is to validate models sufficiently to make believable predictions. The latter requires large datasets of consistent quality and sufficient computational methods and power, while most models of coagulation were developed before the computational tools and large datasets were available.

Here, we have assessed key current mathematical models of coagulation in light of these challenges. We have thoroughly detailed differences in the structure of the reactions that they incorporate and their rates. We then validated the models against a large dataset, providing a thorough investigation into how variations in model structures and rates contribute to variations in thrombin generation predictions. With the aim of improving the understanding of the models and facilitating other groups to carry out their own investigations, we have provided the code, in an open-source language, to run each of the models, making this type of analysis more accessible to a wider audience.

It is worth noting that the data used here encompass both the levels of procoagulants and inhibitors (model inputs) alongside experimentally derived, time-dependent thrombin generation curves (model outputs). It is from a mix of MI patients and healthy matched controls, but there are small but statistically significant differences in the levels of many of the coagulation factors (reported previously [43]) and in the thrombin generation curves in these plasma samples [42]; these all fall within the normal range (Supplementary Figure S2) providing a suitable dataset to test the models. Additionally, thrombin generation is experimentally derived through the cleavage of a chromogenic or fluorogenic substrate, the rate of which is not accounted for in many models. The models also do not account for how the effects of α2-M are subtracted from the data [5], although this could be simulated in models that feature α2-M.

We established that while existing mathematical models of coagulation can predict thrombin generation for some donors, they cannot do this consistently across the dataset. With the exception of the Lakshmanan model, the predictions separate into 2 distinct groups based on the shape of their thrombin generation curves (which we define as "Quick" and "Symmetrical"), neither of which exactly reflect experimentally derived thrombin generation. The inclusion into these groups is predominately based on differing levels of FIX activation, which ultimately depends on the inclusion (or lack of) FXI. Other differences in predictions reflect uncertainty in the underlying biological mechanisms. For example, it is unclear if FIX, FX, and FXI are fully depleted in plasma. This has not been explored experimentally as it has been for prothrombin [47] and could be useful for model validation. Similarly, a better understanding of the mechanisms of AT inhibition of the prothrombinase (Xa:Va) and tenase (IXa:VIIIa) complexes would aid discrimination between accurate and inaccurate model predictions. We found that the wide range of reaction rates utilized in the different models contributes to considerable variation in model predictions of thrombin generation and that this can be caused by just a single reaction rate, as seen in the Chatterjee model for FXI autoactivation and the Bungay model for FIIa inhibition by AT.

We believe the Lakshmanan model is able to reproduce a typical thrombin generation curve shape because its reaction rates were adjusted away from the original experimentally derived values used in Hockin et al. [16] so that the model could better fit new data. Focusing these data on the influence of FXI and low TF may have improved robustness of the thrombin generation curve shape at high TF concentrations.

All presented results use the free thrombin concentration excluding complexes to replicate the conditions of the assay, where free thrombin is calculated as the rate of activation of the chromogenic substrate.

While the models may be unable to reproduce experimental thrombin generation, we believe that they are not without purpose, still being the best tool available to quantify and explore our current understanding of such a complex system. Through comparison to experimental data, they allow fast iterations through possible explanations of discrepancies between model predictions and observations [32]. Given the number of possible interactions in the cascade, a piecemeal approach to validation may be advisable, focusing on subsets of reactions that can be validated before they are combined into a full model. This approach was highlighted in the study by Naski and Shafer [52], where they were able to develop a model for conversion of fibrinogen into fibrin and show that this description accurately reproduced experimental data.

A particular source of variation in the models was found to be the inclusion or exclusion of FXI, which is known to play a role *in vitro* [53,54]. It seems reasonable to conclude that the limited availability of reaction rates for FXI activation, as mentioned in Chatterjee et al. [28], and the large differences in model output driven by the inclusion or exclusion of FXI result in it being a key area of improvement for these models. Recent studies have identified reaction rates for FXI activation by FIIa in the presence of PLs [55], which we expect would be a useful inclusion in the models. Additionally, both the models and the experimentally derived data on thrombin generation rely on a relatively fixed assumption of the contribution of the procoagulant PL surface. New and emerging understanding of the importance of oxidative modifications of PL may have relevance in generating both mathematical and experimental models of thrombin generation that more accurately reflect coagulation as it occurs *in vivo* [56–58].

Our systematic validation of current models of coagulation has highlighted many potential areas for improvement. For example, the models of Hockin, Danforth, and Brummel-Ziedins all lack inclusion of FXI, Bungay lacks FXa activation of FII and has a low rate for FIIa inhibition by AT, and Chatterjee is too sensitive to the effects of FXIa. While these changes could be made, as we have noted, variations in the reaction rates used could still lead to variability in predictions. However, we are at a stage to address such issues. Large cohort data are growing in number, and the computational power and techniques to infer and validate models against such data continue to be developed [59–61]. Indeed, while mathematical models of thrombin generation are not quite there yet, this approach is the essential next step if models of coagulation are to be used to provide detailed and cost-effective explorations of the effects of subtle changes in the hemostatic profile of an individual and ultimately be utilized in the context of precision medicine.

AUTHOR CONTRIBUTIONS

M.J.O. carried out the mathematical modeling, software development, and data analysis. J.L.D. conceived the study and, with A.H.G. and J.R.K., supervised the study. J.R.W. carried out the laboratory analysis. A.H.G. and E.G.D.T. provided advice on hemostasis, and J.R.K. provided mathematical oversight. All authors provided critical review of the manuscript.

DECLARATION OF COMPETING INTERESTS

There are no competing interests to disclose.

DATA AVAILABILITY

A Python translation of the MATLAB code produced in this study, along with instructions on how to use it, is available at the following database: modeling computer scripts: GitHub (https://doi.org/10.5281/zenodo.10523634; https://github.com/mjowen/MathematicalModelsOfCoagulation-AreWeThereYet)

X

Matt J. Owen 𝕏 @MattJOwen_

REFERENCES

[1] Mohammed BM, Matafonov A, Ivanov I, Sun MF, Cheng Q, Dickeson SK, Li C, Sun D, Verhamme IM, Emsley J, Gailani D. An update on factor XI structure and function. *Thromb Res*. 2018;161:94–105.

[2] Danforth CM, Orfeo T, Everse SJ, Mann KG, Brummel-Ziedins KE. Defining the boundaries of normal thrombin generation: investigations into hemostasis. *PLoS One*. 2012;7:e30385.

[3] Hemker HC, Wielders S, Kessels H, Béguin S. Continuous registration of thrombin generation in plasma, its use for the determination of the thrombin potential. *Thromb Haemost*. 1993;70:617–24.

[4] Hemker HC, Giesen P, Al Dieri R, Regnault V, de Smedt E, Wagenvoord R, Lecompte T, Béguin S. Calibrated automated thrombin generation measurement in clotting plasma. *Pathophysiol Haemost Thromb*. 2003;33:4–15.

[5] Hemker HC, Kremers R. Data management in thrombin generation. *Thromb Res*. 2013;131:3–11.

[6] Hoffman M, Monroe DM. A cell-based model of hemostasis. *Thromb Haemost*. 2001;85:958–65.

[7] Ninivaggi M, de Laat-Kremers RMW, Carlo A, de Laat B. ST Genesia reference values of 117 healthy donors measured with STG-BleedScreen, STG-DrugScreen and STG-ThromboScreen reagents. *Res Pract Thromb Haemost*. 2021;5:187–96.

[8] de Laat-Kremers R, Zuily S, de Laat B. Editorial: advances in thrombin generation. *Front Cardiovasc Med*. 2023;10:1183718.

[9] Khanin MA, Semenov VV. A mathematical model of the kinetics of blood coagulation. *J Theor Biol*. 1989;136:127–34.

[10] Willems GM, Lindhout T, Hermens WT, Hemker HC. Simulation model for thrombin generation in plasma. *Haemostasis*. 1991;21:197–207.

[11] Jones KC, Mann KG. A model for the tissue factor pathway to thrombin. II. A mathematical simulation. *J Biol Chem*. 1994;269:23367–73.

[12] Leipold RJ, Bozarth TA, Racanelli AL, Dicker IB. Mathematical model of serine protease inhibition in the tissue factor pathway to thrombin. *J Biol Chem*. 1995;270:25383–7.

[13] Zarnitsina VI, Pokhilko AV, Ataullakhanov FI. A mathematical model for the spatio-temporal dynamics of intrinsic pathway of blood coagulation. I. The model description. *Thromb Res*. 1996;84:225–36.

[14] Khanin MA, Rakov DV, Kogan AE. Mathematical model for the blood coagulation prothrombin time test. *Thromb Res*. 1998;89:227–32.

[15] Kuharsky AL, Fogelson AL. Surface-mediated control of blood coagulation: the role of binding site densities and platelet deposition. *Biophys J*. 2001;80:1050–74.

[16] Hockin MF, Jones KC, Everse SJ, Mann KG. A model for the stoichiometric regulation of blood coagulation. *J Biol Chem*. 2002;277:18322–33.

[17] Xu CQ, Zeng YJ, Gregersen H. Dynamic model of the role of platelets in the blood coagulation system. *Med Eng Phys*. 2002;24:587–93.

[18] Bungay SD, Gentry PA, Gentry RD. A mathematical model of lipid-mediated thrombin generation. *Math Med Biol*. 2003;20:105–29.

[19] Butenas S, Orfeo T, Gissel MT, Brummel KE, Mann KG. The significance of circulating factor IXa in blood. *J Biol Chem*. 2004;279:22875–82.

[20] Qiao YH, Liu JL, Zeng YJ. A kinetic model for simulation of blood coagulation and inhibition in the intrinsic path. *J Med Eng Technol*. 2005;29:70–4.

[21] Xu C, Xu XH, Zeng Y, Chen YW. Simulation of a mathematical model of the role of the TFPI in the extrinsic pathway of coagulation. *Comput Biol Med*. 2005;35:435–45.

[22] Tyurin KV, Khanin MA. Hemostasis as an optimal system. *Math Biosci*. 2006;204:167–84.

[23] Panteleev MA, Ovanesov MV, Kireev DA, Shibeko AM, Sinauridze EI, Ananyeva NM, Butylin AA, Saenko EL, Ataullakhanov FI. Spatial propagation and localization of blood coagulation are regulated by intrinsic and protein C pathways, respectively. *Biophys J*. 2006;90:1489–500.

[24] Zhu D. Mathematical modeling of blood coagulation cascade: kinetics of intrinsic and extrinsic pathways in normal and deficient conditions. *Blood Coagul Fibrinolysis*. 2007;18:637–46.

[25] Luan D, Zai M, Varner JD. Computationally derived points of fragility of a human cascade are consistent with current therapeutic strategies. *PLoS Comput Biol*. 2007;3:e142.

[26] Danforth CM, Orfeo T, Mann KG, Brummel-Ziedins KE, Everse SJ. The impact of uncertainty in a blood coagulation model. *Math Med Biol*. 2009;26:323–36.

[27] Panteleev MA, Balandina AN, Lipets EN, Ovanesov MV, Ataullakhanov FI. Task-oriented modular decomposition of biological networks: trigger mechanism in blood coagulation. *Biophys J*. 2010;98:1751–61.

[28] Chatterjee MS, Denney WS, Jing H, Diamond SL. Systems biology of coagulation initiation: kinetics of thrombin generation in resting and activated human blood. *PLoS Comput Biol*. 2010;6:e1000950.

[29] Brummel-Ziedins KE, Orfeo T, Callas PW, Gissel M, Mann KG, Bovill EG. The prothrombotic phenotypes in familial protein C deficiency are differentiated by computational modeling of thrombin generation. *PLoS One*. 2012;7:e44378.

[30] Mitrophanov AY, Szlam F, Sniecinski RM, Levy JH, Reifman J. A step toward balance: thrombin generation improvement via procoagulant factor and antithrombin supplementation. *Anesth Analg*. 2016;123:535–46.

[31] Lakshmanan HHS, Estonilo A, Reitsma SE, Melrose AR, Subramanian J, Zheng TJ, Maddala J, Tucker EI, Gailani D, McCarty OJT, Jurney PL, Puy C. Revised model of the tissue factor pathway of thrombin generation: role of the feedback activation of FXI. *J Thromb Haemost*. 2022;20:1350–63.

[32] Stobb MT, Monroe DM, Leiderman K, Sindi SS. Assessing the impact of product inhibition in a chromogenic assay. *Anal Biochem*. 2019;580:62–71.

[33] Link KG, Stobb MT, Sorrells MG, Bortot M, Ruegg K, Manco-Johnson MJ, Di Paola JA, Sindi SS, Fogelson AL, Leiderman K, Neeves KB. A mathematical model of coagulation under flow

identifies factor V as a modifier of thrombin generation in hemophilia A. *J Thromb Haemost*. 2020;18:306–17.
[34] Link KG, Stobb MT, Di Paola J, Neeves KB, Fogelson AL, Sindi SS, Leiderman K. A local and global sensitivity analysis of a mathematical model of coagulation and platelet deposition under flow. *PLoS One*. 2018;13:e0200917.
[35] Méndez Rojano R, Mendez S, Lucor D, Ranc A, Giansily-Blaizot M, Schved JF, Nicoud F. Kinetics of the coagulation cascade including the contact activation system: sensitivity analysis and model reduction. *Biomech Model Mechanobiol*. 2019;18:1139–53.
[36] Grande Gutiérrez N, Mukherjee D, Bark D Jr. Decoding thrombosis through code: a review of computational models. *J Thromb Haemost*. 2024;22:35–47.
[37] Brummel-Ziedins KE, Orfeo T, Gissel M, Mann KG, Rosendaal FR. Factor Xa generation by computational modeling: an additional discriminator to thrombin generation evaluation. *PLoS One*. 2012;7:e29178.
[38] Siekmann I, Bjelosevic S, Landman K, Monagle P, Ignjatovic V, Crampin EJ. Mathematical modelling indicates that lower activity of the haemostatic system in neonates is primarily due to lower prothrombin concentration. *Sci Rep*. 2019;9:3936.
[39] Mann KG. Is there value in kinetic modeling of thrombin generation? Yes. *J Thromb Haemost*. 2012;10:1463–9.
[40] Hemker HC, Kerdelo S, Kremers RMW. Is there value in kinetic modeling of thrombin generation? No (unless...). *J Thromb Haemost*. 2012;10:1470–7.
[41] Chelle P, Morin C, Montmartin A, Piot M, Cournil M, Tardy-Poncet B. Evaluation and calibration of in silico models of thrombin generation using experimental data from healthy and haemophilic subjects. *Bull Math Biol*. 2018;80:1989–2025.
[42] Brouilette S, Singh RK, Thompson JR, Goodall AH, Samani NJ. White cell telomere length and risk of premature myocardial infarction. *Arterioscler Thromb Vasc Biol*. 2003;23:842–6.
[43] Dunster JL, Wright JR, Samani NJ, Goodall AH. A system-wide investigation and stratification of the hemostatic proteome in premature myocardial infarction. *Front Cardiovasc Med*. 2022;9:919394.
[44] Zekavat OR, Haghpanah S, Dehghani J, Afrasiabi A, Peyvandi F, Karimi M. Comparison of thrombin generation assay with conventional coagulation tests in evaluation of bleeding risk in patients with rare bleeding disorders. *Clin Appl Thromb Hemost*. 2014;20:637–44.
[45] Rios DRA, Barreto SM, Ferreira LGR, Batista TR, Silva APF, de Oliveira Júnior WV, Maluf CB, Carvalho MDG, Figueiredo RC. Performance and reference intervals of thrombin generation test: results from the Brazilian longitudinal study of adult health (ELSA-Brasil). A cross-sectional study. *Sao Paulo Med J*. 2022;140:474–85.
[46] Campello E, Bulato C, Spiezia L, Boscolo A, Poletto F, Cola M, Gavasso S, Simion C, Radu CM, Cattelan A, Tiberio I, Vettor R, Navalesi P, Simioni P. Thrombin generation in patients with COVID-19 with and without thromboprophylaxis. *Clin Chem Lab Med*. 2021;59:1323–30.
[47] Kremers RMW, Peters TC, Wagenvoord RJ, Hemker HC. The balance of pro- and anticoagulant processes underlying thrombin generation. *J Thromb Haemost*. 2015;13:437–47.
[48] Al Dieri R, Bloemen S, Kelchtermans H, Wagenvoord R, Hemker HC. A new regulatory function of activated factor V: inhibition of the activation by tissue factor/factor VII(a) of factor X. *J Thromb Haemost*. 2013;11:503–11.
[49] Castoldi E, Simioni P, Tormene D, Rosing J, Hackeng TM. Hereditary and acquired protein S deficiencies are associated with low TFPI levels in plasma. *J Thromb Haemost*. 2010;8:294–300.
[50] Reglińska-Matveyev N, Andersson HM, Rezende SM, Dahlbäck B, Crawley JTB, Lane DA, Ahnström J. TFPI cofactor function of protein S: essential role of the protein S SHBG-like domain. *Blood*. 2014;123:3979–87.
[51] Ahnström J, Andersson HM, Hockey V, Meng Y, McKinnon TAJ, Hamuro T, Crawley JT, Lane DA. Identification of functionally important residues in TFPI Kunitz domain 3 required for the enhancement of its activity by protein S. *Blood*. 2012;120:5059–62.
[52] Naski MC, Shafer JA. A kinetic model for the α-thrombin-catalyzed conversion of plasma levels of fibrinogen to fibrin in the presence of antithrombin III. *J Biol Chem*. 1991;266:13003–10.
[53] Gailani D, Broze GJ. Factor XI activation in a revised model of blood coagulation. *Science*. 1991;253:909–12.
[54] Naito K, Fujikawa K. Activation of human blood coagulation factor XI independent of factor XII. Factor XI is activated by thrombin and factor XIa in the presence of negatively charged surfaces. *J Biol Chem*. 1991;266:7353–8.
[55] Omarova F, Rosing J, Bertina RM, Castoldi E. Negatively charged phospholipids stimulate factor XI activation by thrombin. *Thromb Update*. 2021;2:100022.
[56] Protty MB, Jenkins PV, Collins PW, O'Donnell VB. The role of procoagulant phospholipids on the surface of circulating blood cells in thrombosis and haemostasis. *Open Biol*. 2022;12:210318.
[57] Thomas CP, Morgan LT, Maskrey BH, Murphy RC, Kühn H, Hazen SL, Goodall AH, Hamali HA, Collins PW, O'Donnell VB. Phospholipid-esterified eicosanoids are generated in agonist-activated human platelets and enhance tissue factor-dependent thrombin generation. *J Biol Chem*. 2010;285:6891–903.
[58] Clark SR, Thomas CP, Hammond VJ, Aldrovandi M, Wilkinson GW, Hart KW, Murphy RC, Collins PW, O'Donnell VB. Characterization of platelet aminophospholipid externalization reveals fatty acids as molecular determinants that regulate coagulation. *Proc Natl Acad Sci U S A*. 2013;110:5875–80.
[59] Sunnåker M, Busetto AG, Numminen E, Corander J, Foll M, Dessimoz C. Approximate Bayesian computation. *PLoS Comput Biol*. 2013;9:e1002803.
[60] Ghosh S, Dasmahapatra S, Maharatna K. Fast approximate Bayesian computation for estimating parameters in differential equations. *Stat Comput*. 2017;27:19–38.
[61] Everitt RG, Rowińska PA. Delayed acceptance ABC-SMC. *J Comput Graph Stat*. 2021;30:55–66.

SUPPLEMENTARY MATERIAL

The online version contains supplementary material available at https://doi.org/10.1016/j.jtha.2024.03.009